

# Temperature Dependence of the Intrinsic Anomalous Hall Effect in Nickel

Li Ye, Yuan Tian, and Xiaofeng Jin\*

*State Key Laboratory of Surface Physics and Department of Physics, Fudan University, Shanghai 200433, China*

Di Xiao

*Materials Science and Technology Division, Oak Ridge National Laboratory, Oak Ridge, TN 37831, USA*

(Dated: January 26, 2013)

We investigate the unusual temperature dependence of the anomalous Hall effect in Ni. By varying the thickness of the MBE-grown Ni films, the longitudinal resistivity is uniquely tuned without resorting to doping impurities; consequently, the intrinsic and extrinsic contributions are cleanly separated out. In stark contrast to other ferromagnets such as Fe, the intrinsic contribution in Ni is found to be strongly temperature dependent with a value of  $1100 (\Omega \cdot \text{cm})^{-1}$  at low temperatures and  $500 (\Omega \cdot \text{cm})^{-1}$  at high temperatures. This pronounced temperature dependence, a cause of long-standing confusion concerning the physical origin of the AHE, is likely due to the small energy level splitting caused by the spin orbit coupling close to the Fermi surface. Our result helps pave the way for the general claim of the Berry-phase interpretation for the AHE.

PACS numbers: 71.70.Ej;72.15.Eb;73.50.Jt;75.47.Np

Recent years have seen a surge of renewed interest in the anomalous Hall effect (AHE) in ferromagnets, largely driven by its close relation to various spintronic applications[1]. It is now firmly established that there are several competing mechanisms contributing to the AHE. One is the extrinsic mechanism based on the modified impurity scattering in the presence of the spin-orbit coupling (SOC), i.e., the skew scattering and the side jump mechanism[2, 3]. The other stems from the anomalous velocity of the Bloch electrons induced by the SOC, originally proposed by Karplus and Luttinger[4]. This contribution can be interpreted in terms of the Berry curvature of occupied Bloch states, and is of intrinsic nature[5–7]. Both recent experiments and theoretical calculations seem to suggest that the intrinsic contribution is dominant in moderately conducting samples of itinerant ferromagnets[8–11].

Despite the latest success of the Berry-phase interpretation, it comes as a surprise that the physical origin of the AHE in Ni, one of the simplest yet most important itinerant ferromagnets, is still unresolved. The main problem lies in the complicated temperature dependence of the AHE in this material, which prevents a clear identification of different contributions. Smit first reported a power law scaling between the anomalous Hall resistivity  $\rho_{\text{AH}}$  and the longitudinal resistivity  $\rho_{xx}$  with  $\rho_{\text{AH}} \propto \rho_{xx}^{1.4}$  in Ni[2], which does not fit either the extrinsic or the intrinsic scenario. This situation is further complicated by the strong temperature dependence of the scaling observed by Lavine[12], with  $\rho_{\text{AH}} \propto \rho_{xx}^{1.10}$  at low temperatures below 150 K,  $\rho_{\text{AH}} \propto \rho_{xx}^{1.97}$  at high temperatures around 300 K, and  $\rho_{\text{AH}} \propto \rho_{xx}^{1.70}$  in between. At even lower temperature (4.2 K), Fert *et al.* found a linear relation of  $\rho_{\text{AH}} \propto \rho_{xx}$  by varying the impurity concentration in their high quality Ni single crystal samples ( $\rho_{xx} < 1 \mu\Omega \cdot \text{cm}$ ), which is a clear indication of the ex-

trinsic skew scattering mechanism[13]. Theoretical investigations have not provided much insight either. Large discrepancy was found between first-principles calculations of the intrinsic AHE and experiments[14]. This is in sharp contrast to other itinerant ferromagnets such as Fe and Co, where agreement within better than 30% has been found and the dominance of the intrinsic mechanism is clearly established[8, 11, 15].

In this Letter we examine the temperature dependence of the AHE in Ni thin films with varying thickness. This approach allows us to tune the resistivity  $\rho_{xx}$  without modifying the impurity concentration. We are able to extract, for the first time, the intrinsic anomalous Hall conductivity in Ni, and demonstrate quantitatively its dominance. Surprisingly, the intrinsic AHE is strongly temperature dependent over a large range (5 to 150 K) in which the magnetization stays almost the same. This is different from the previously studied cases where the temperature dependence is explained by changes in the magnetization[16, 17]. We attribute the strong temperature dependence to the complex Fermi surface of Ni in the presence of the SOC. Our result not only clears up the long-standing puzzle of the physical origin of the AHE in Ni, but also paves the way for the general claim of the Berry-phase interpretation for the AHE.

Ni films with thickness from 6 to 30 nm were epitaxially grown on MgO(001) by molecular beam epitaxy with its orientation relative to the substrate, Ni[001]||MgO[001] and Ni[100]||MgO[100]; the detailed experimental setup was described elsewhere[18]. Clean and ordered MgO(001) surface was first prepared by annealing at 1100 K in UHV, on which the epitaxial growth of Ni at 300 K was then followed. Using an in-situ mask, we have prepared films with several different thicknesses on the same substrate. They were further annealed at 600 K for 1 hour to acquire better crystal quality and

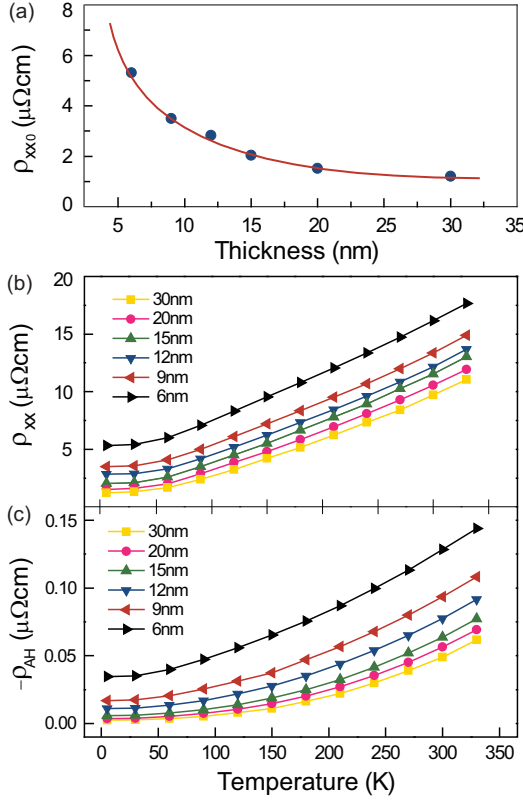


FIG. 1: (a) Thickness dependence of  $\rho_{xx0}$  with red guide-line for eyes. Inset: RHEED pattern for 30nm thick Ni film, with incident electron along MgO [100]. (b), (c) Temperature dependence of  $\rho_{xx}$  and  $\rho_{AH}$  for various film thicknesses.

surface morphology[19]. A representative reflection high energy electron diffraction (RHEED) pattern after annealing is shown in the inset of Fig. 1(a). The improved sample quality after the annealing was also revealed from the significant decreasing ( $> 50\%$ ) of the corresponding sample residual resistivity  $\rho_{xx0}$ . Meanwhile, the magnetization monitored by the magneto-optic Kerr effect (MOKE) remained almost the same, which indicated that the interface diffusion between Ni and MgO was negligible during the annealing. In order to prevent oxidation in the ambient air during the transport measurement, a capping layer of 5 nm MgO was further deposited on top of Ni before each sample was taken out from the UHV chamber. The films were then patterned into the form of a standard Hall bar along [100] with the magnetic field along the [001] direction, and the anomalous Hall resistivity  $\rho_{AH}$  and the longitudinal resistivity  $\rho_{xx}$  were simultaneously measured with the physical property measurement system (PPMS-9T).

Figure 1(a) shows the residual resistivity  $\rho_{xx0}$  of Ni (measured at 5 K) as a function of film thickness ranging from 6 to 30 nm, where a factor of five-fold decrease is observed. This is due to the finite size effect in electrical resistivity of thin metallic films induced by the geomet-

rical limitation of the bulk (or background) mean free path of conduction electrons[20]. The current selection of film thicknesses allows us to change the impurity scattering with little alteration of the bulk electronic structure [21, 22].

Figure 1(b) and (c) show the temperature dependence of both  $\rho_{xx}$  and  $\rho_{AH}$  for different film thicknesses, respectively. The negative sign of  $\rho_{AH}$  reflects the fact that the chirality of the AHE in Ni is opposite to that of Fe [11]. We plot  $\rho_{AH}$  as a function of  $\rho_{xx}$  for the thickest 30 nm Ni film in Fig. 2(a). The  $\rho_{AH} = f(\rho_{xx})$  curve agrees well with previous observations for the temperature-dependent scaling of the AHE in bulk Ni [12]. As mentioned earlier, it is exactly this complicated scaling that makes the intrinsic origin of the AHE in Ni rather elusive.

We now try to separate the different contributions to the AHE by applying the scaling law proposed in our recent work, in which we have shown that the extrinsic contribution should be scaled against the residual resistivity  $\rho_{xx0}$  instead of the total resistivity  $\rho_{xx}$ . This leads to the following scaling relation[11]:

$$\sigma_{AH} = -(\alpha\sigma_{xx0}^{-1} + \beta\sigma_{xx0}^{-2})\sigma_{xx}^2 - b, \quad (1)$$

where  $\alpha$ ,  $\beta$ , and  $b$  are constants to be determined from the fitting, and  $\sigma_{AH}$ ,  $\sigma_{xx0}$ , and  $\sigma_{xx}$  are the anomalous Hall conductivity, residual and total longitudinal conductivity, respectively. Here, the first and last terms represent the extrinsic skew scattering and the intrinsic Berry phase contributions respectively, while the  $\beta$  term is clearly extrinsic and was previously ascribed to the side-jump contribution. Figure 2(b) shows  $\sigma_{AH}$  as a function of  $\sigma_{xx}^2(T)$  from 5 to 330 K for different film thicknesses. It is observed, as anticipated, that when  $\sigma_{xx}^2(T)$  goes to zero, the anomalous Hall conductivity  $\sigma_{AH}$  for various film thicknesses with different residual resistivity converges to a universal value  $500\Omega^{-1}\text{cm}^{-1}$ , reflecting unambiguously the intrinsic nature of the AHE at the high temperature limit. However, for a given thickness, significant deviation from a linear scaling between  $\sigma_{AH}$  and  $\sigma_{xx}^2(T)$  are clearly noticeable, which suggests that the scaling in Eq. (1) does not apply directly to the AHE in Ni, if  $\alpha$ ,  $\beta$  and  $b$  were to be fixed at constant values.

To remedy this situation, we propose a generic scaling

$$\sigma_{AH} = -(\alpha\sigma_{xx0}^{-1} + \beta\sigma_{xx0}^{-2})\sigma_{xx}^2 - b(T), \quad (2)$$

or equivalently

$$\rho_{AH} = (\alpha\rho_{xx0} + \beta\rho_{xx0}^2) + b(T)\rho_{xx}^2, \quad (3)$$

where  $\alpha$  and  $\beta$  are still constants, but  $b(T)$ , which represents the intrinsic Berry-phase contribution, is now a function of temperature. Recall that the magnetocrystalline anisotropy of Ni is strongly temperature dependent between 5 and 330 K[23]. It is thus reasonable to anticipate that the Berry-phase contribution to the

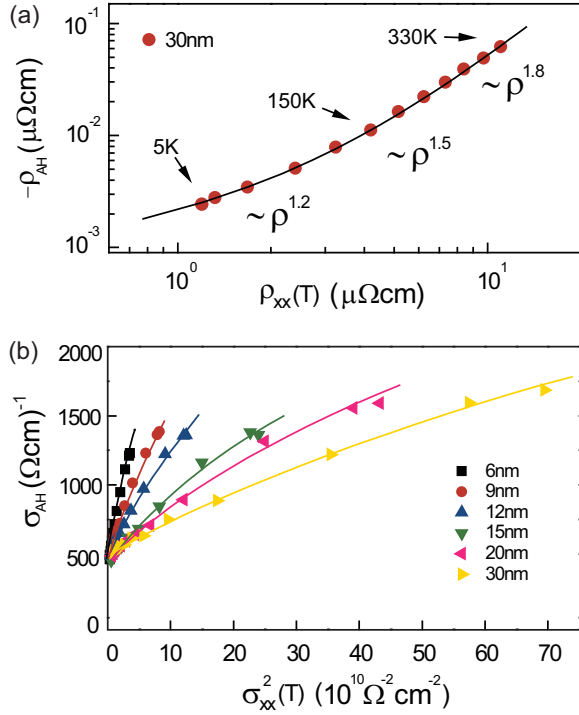


FIG. 2: (a)  $\rho_{AH}$  v.s.  $\rho_{xx}(T)$  plot in logarithmic scale for 30nm-Ni showing temperature dependent power law. (b)  $\sigma_{AH}$  v.s.  $\sigma_{xx}^2(T)$  plot for various film thicknesses.

AHE, which originates from the SOC in the band structure, is also temperature-dependent. Therefore, instead of analyzing the scaling  $\rho_{AH} = f(\rho_{xx}(T))$  with varying temperature for each fixed film thickness, we should consider the same scaling but with varying film thickness for each fixed temperature  $\rho_{AH} = f(\rho_{xx}(d))$ .

We first consider the low-temperature limit. At 5 K, the phonon scattering is negligible and the scaling relation in Eq. (3) reduces to  $\rho_{AH0} = \alpha\rho_{xx0} + (\beta + b_0)\rho_{xx0}^2$ , where  $b_0 = b$  ( $T = 5K$ ) is a constant for different film thickness. Figure 3(a) shows the  $\rho_{AH0}/\rho_{xx0}(d)$  v.s.  $\rho_{xx0}(d)$  plot, using the set of 5 K data in Fig. 1(b) and (c). From the nice linear fitting by the black line as shown in the figure, we obtain the skew scattering constant  $\alpha = -7 \times 10^{-4}$  directly from the intercept, which is comparable with the value (on the order of  $10^{-3}$  depending on impurity type) previously obtained by Fert *et al*[13].

Now the scaling can be recast into  $\rho_{AH} - \alpha\rho_{xx0} = \beta\rho_{xx0}^2 + b(T)\rho_{xx}^2$ , and Fig. 3(b) shows the new set of plots  $\rho_{AH}(d) - \alpha\rho_{xx0}(d)$  v.s.  $\rho_{xx}^2(d)$  with varying film thickness for each fixed temperature ranging from 5 to 330 K. It is clear that at each given temperature all the experimental data can indeed be well described by the generic scaling, as they are all nicely fitted by the straight lines in the whole temperature range. In addition, it is found that  $\beta \approx 0$  in the specific MgO/Ni/MgO system, while it can be tuned to nonzero for different interfaces (not shown

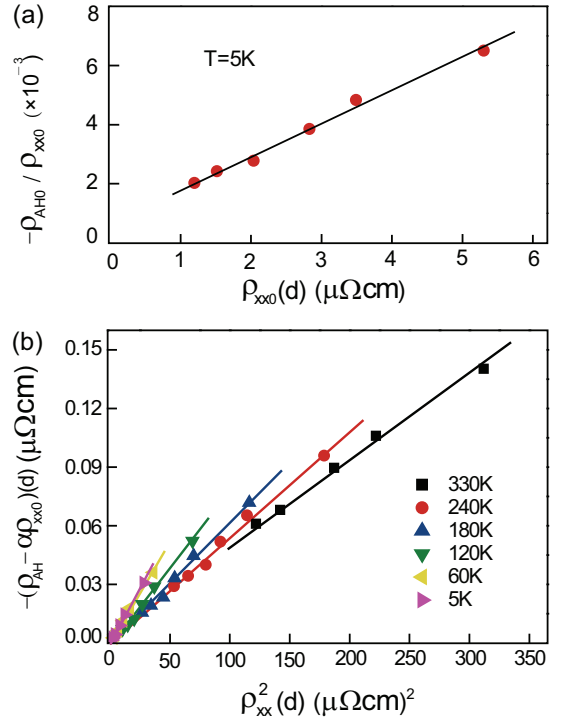


FIG. 3: (a)  $\rho_{AH0}/\rho_{xx0}(d)$  v.s.  $\rho_{xx0}(d)$  plot. (b)  $\rho_{AH}(d) - \alpha\rho_{xx0}(d)$  v.s.  $\rho_{xx}^2(d)$  plot at various temperatures.

here).

The different slopes in Fig. 3(b) at each given temperature give the intrinsic temperature-dependent anomalous Hall conductivity  $\sigma_{\text{int}}(T) = -b(T)$  in Ni, which are shown in Fig. 4, marked by solid (green) circle.  $\sigma_{\text{int}}(T)$  is about  $1100 (\Omega \cdot \text{cm})^{-1}$  at low temperature, and decreases to about  $500 (\Omega \cdot \text{cm})^{-1}$  when the temperature is above 300 K. It becomes transparent now that it is this temperature dependent intrinsic term that has caused all the earlier complications and confusions in understanding the AHE in Ni. It should be pointed out that this term cannot be singled out from the AHE measurements on a single Ni sample. Instead, it is only possible on a series of samples with tunable residual resistivity  $\rho_{xx0}$  while keeping their electronic band structures basically the same, otherwise the corresponding Berry curvatures would be different from each other. This argument also explains why the previous approaches by adding impurities in Ni have all failed to unveil the intrinsic origin for the AHE in Ni.

To better understand the microscopic mechanisms of the AHE in bulk Ni, we also show in Fig. 4 the raw data (red square dots) of the experimentally measured anomalous Hall conductivity  $\sigma_{AH}^{30nm}$  in the bulk-like 30 nm Ni film. Using the aforementioned result of  $\alpha = -7 \times 10^{-4}$  we can plot the temperature dependent skew scattering conductivity  $\sigma_{sk}^{30nm} = -\alpha\sigma_{xx0}^{-1}\sigma_{xx}^2(T)$  for this bulk-like 30 nm Ni film, shown as blue triangles in Fig. 4(a). Now subtracting  $\sigma_{sk}^{30nm}$  from  $\sigma_{AH}^{30nm}$ , we obtain the intrinsic

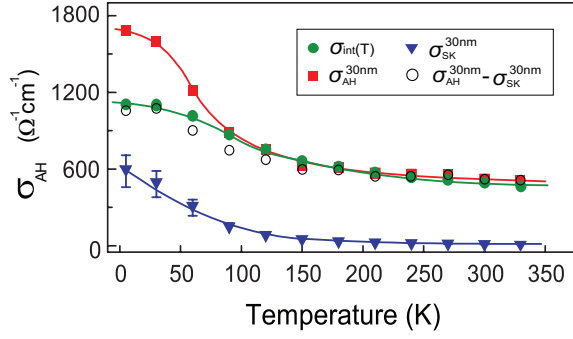


FIG. 4: Temperature dependence of  $\sigma_{\text{int}}$  in Ni together with various contributions in 30nm thick Ni; the solid curves are guidelines for eyes.

anomalous Hall conductivity in this 30 nm Ni film, as given by the open circles in Fig. 4(a). It should be emphasized that  $\sigma_{\text{int}}(T)$  and  $\alpha = -7 \times 10^{-4}$  are obtained from a series of samples with different film thicknesses (not necessary to include the data from the 30 nm Ni film) while  $\sigma_{\text{AH}}^{30\text{nm}} - \sigma_{\text{sk}}^{30\text{nm}}$  is for a single film thickness. The excellent agreement between  $\sigma_{\text{int}}(T)$  and  $\sigma_{\text{AH}}^{30\text{nm}} - \sigma_{\text{sk}}^{30\text{nm}}$  clearly reflects the consistency of the overall analysis adopted here. In addition, it can be seen clearly from Fig. 4 that the intrinsic contribution dominates in the whole temperature range 5 to 300 K.

The temperature dependence of the intrinsic AHE can be understood from the existence of degenerate or nearly degenerate bands near the Fermi surface in Ni. It is well known that in Ni the minority spin bands have small hole pockets around  $X$ [24]. These bands are of  $t_{2g}$  character and are doubly degenerate in the absence of the SOC. With SOC, this degeneracy is lifted, resulting in large value of the Berry curvature[25]. Given the close proximity of these bands to the Fermi surface, they will be thermally populated at finite temperatures. First-principles calculations indicate that contributions to the AHE from these hole pockets are opposite in sign [14], which explains why  $\sigma_{\text{int}}(T)$  decreases with increasing temperature. Similar behavior has also been observed in first-principles calculation of the spin Hall effect in Pt [26].

With our new insight on the AHE in Ni, we now clarify the earlier confusions and complications in literatures. Given the values of  $\sigma_{\text{int}}(5\text{ K}) = 1100 (\Omega \cdot \text{cm})^{-1}$  and  $\alpha = -7 \times 10^{-4}$ , the skew scattering term  $\rho_{\text{sk}} = \alpha \rho_{xx0}$  is expected to overwhelm the intrinsic one  $\rho_{\text{int}} = -\sigma_{\text{int}} \rho_{xx}^2$  if the residual resistivity  $\rho_{xx0}$  is below  $0.5 \mu\Omega \cdot \text{cm}$ , which corresponds to the so called "clean limit" in the AHE where the linear term  $\rho_{\text{AH}0} = \alpha \rho_{xx0}$  dominates. This

explains why in the ultra-pure Ni samples at low temperature, Fert et al., did observe an overall linear scaling  $\rho_{\text{AH}0} = \alpha \rho_{xx0}$ . On the other hand, the temperature dependent power law scaling  $\rho_{xx}^n$  or the average power law  $\rho_{xx}^{1.4}$  are in fact some ill-defined average of the real scaling  $\rho_{\text{AH}} = \alpha \rho_{xx0} + \beta \rho_{xx0}^2 - \sigma_{\text{int}}(T) \rho_{xx}^2$ . Finally, so far first-principles calculations of the intrinsic AHE have been compared to 320 to 750  $(\Omega \cdot \text{cm})^{-1}$  measured at room temperature[2, 12]. Our result shows that for zero-temperature calculation, one should compare to  $\sigma_{\text{int}}(5\text{ K}) = 1100 (\Omega \cdot \text{cm})^{-1}$ .

The authors thank G. Malcolm Stocks for useful discussions on the band structure of Ni. This work was supported by MOST (No. 2009CB929203), NSFC (No. 10834001), and SCST. D.X. acknowledges support from the Division of Materials Sciences and Engineering, Office of Basic Energy Sciences, U.S. Department of Energy.

---

\* Corresponding author. xfjin@fudan.edu.cn

- [1] D. Nagaosa et al., Rev. Mod. Phys. 82, 1539 (2010).
- [2] J. Smit, Physica (Amsterdam) 21, 877 (1955).
- [3] L. Berger, Phys. Rev. B 2, 4559 (1970).
- [4] R. Karplus and J. M. Luttinger, Phys. Rev. 95, 1154 (1954); J. M. Luttinger, Phys. Rev. 112, 739 (1958).
- [5] T. Jungwirth et al., Phys. Rev. Lett. 88, 207208 (2002).
- [6] M. Onoda and N. Nagaosa, J. Phys. Soc. Jpn. 71, 19 (2002).
- [7] D. Xiao et al., Rev. Mod. Phys. 82, 1959 (2010).
- [8] Y. Yao et al., Phys. Rev. Lett. 92, 037204 (2004).
- [9] R. Mathieu et al., Phys. Rev. Lett. 93, 016602 (2004).
- [10] T. Miyasato et al., Phys. Rev. Lett. 99, 086602 (2007).
- [11] Y. Tian et al., Phys. Rev. Lett. 103, 087206 (2009).
- [12] J. M. Lavine, Phys. Rev. 123, 1273 (1961).
- [13] A. Fert et al., Phys. Rev. Lett. 28, 303 (1972).
- [14] X. J. Wang et al., Phys. Rev. B 76, 195109 (2007).
- [15] E. Roman et al., Phys. Rev. Lett. 103, 097203 (2009).
- [16] F. Zhong et al., Science 302, 92 (2003).
- [17] C. G. Zeng et al., Phys. Rev. Lett. 96, 037204 (2006).
- [18] C. S. Tian et al., Phys. Rev. Lett. 94, 137210 (2005); L. F. Yin et al., Phys. Rev. Lett. 97, 067203 (2006).
- [19] R. Lukaszewa et al., Appl. Surf. Sci. 219, 74-79 (2003).
- [20] C. R. Tellier and A. J. Tosser, Size Effects in Thin Films (Elsevier, Amsterdam, 1982).
- [21] R. J. Zhang and R. F. Willis, Phys. Rev. Lett. 86, 2665 (2001).
- [22] M. Hoesch et al, Phys. Rev. B. 79, 155404 (2009).
- [23] W. J. Carr, Phys. Rev. 109, 1971 (1958).
- [24] C. S. Wang and J. Callaway, Phys. Rev. B 9, 4897 (1974).
- [25] S. Onoda et al., Phys. Rev. Lett. 97, 126602 (2006).
- [26] G. Y. Guo et al., Phys. Rev. Lett 100, 096401 (2008).